JACS
JOURNAL OF THE AMERICAN CHEMICAL SOCIETY

Communication

pubs.acs.org/JACS

Site-Specific Immobilization of Single-Walled Carbon Nanotubes onto Single and One-Dimensional DNA Origami

Anshuman Mangalum,[§] Masudur Rahman,*[,§] and Michael L. Norton

Department of Chemistry, Marshall University, Huntington, West Virginia 25755, United States

Supporting Information

ABSTRACT: Development of a simple and efficient methodology to control the placement, spacing, and alignment of single-walled carbon nanotubes (SWCNTs) is essential for nanotechnology device application. Building on the growing understanding that the strong $\pi-\pi$ interaction between the bases of single-stranded DNA (ssDNA) and CNTs is sufficient not only to drive CNT solubility in water but also to stabilize individual nanotubes against clustering in aqueous solution, a new motif for functionalizing DNA origami (DO) with CNTs is demonstrated. CNTs solubilized via wrapping with ssDNA react with DO constructs displaying linear arrays of ssDNA, leading to immobilization of the CNTs onto the DO scaffold. This study demonstrates the immobilization of ssDNA-wrapped CNTs at specific positions on single DO constructs. Furthermore, multiple DO constructs assembled into extended one-dimensional arrays have been used to successfully align pairs of CNTs exceeding 500 nm in length in a parallel orientation. This result provides a simplified, alternative approach to immobilization of CNTs with programmed spacing and orientation.

Since their discovery in the early 1990s,[1] single-walled carbon nanotubes (SWCNTs) have become one of the most attractive known allotropes of carbon due to their extraordinarily low density, high tensile strength, and unique thermal, electrical, and optical properties.[2] SWCNTs are essentially graphene sheets rolled into a hollow cylindrical shape; they are particularly remarkable for the tunablility of their physical properties based on the type of tube that is formed. Notable is the potential for very high aspect ratio. Nanometer-diameter tubes with lengths as long as 18.5 cm can be grown.[3] Based on helicity and diameter, CNTs can be semiconductors or metallic, as desired for different applications.[4] Semiconductor CNTs are used as components for charge-transfer applications in sensors, solar cells, and field emission displays, whereas metallic CNTs can also be used in electronic devices and as fillers in CNT composite materials.[5] The solubility of CNTs in common solvents, and the clustering and formation of aggregates due to $\pi-\pi$ interactions, are major barriers to harnessing CNTs' properties to the fullest. Aggregation of unmodified CNTs leads to changes in optical and electronic properties and hence impedes practical applications.[6]

Concurrent with these challenges and advancements in CNT chemistry, DNA-based nanotechnology has been gaining importance due to its wide range of applications in fields of science including medicine, chemistry, energy, communications, physical science, and materials science.[7] In the past decade, a scaffolded DNA nanoarchitecture called "DNA origami" (DO) has opened a new domain for the design and formation of numerous two-dimensional nanostructures.[8] Such DNA structures provide flexible platforms that, through simple modifications, can accommodate various biologically relevant molecules such as proteins[9] and enzymes[10] or other functional materials such as metal nanoparticles,[11] quantum dots,[12] and, as shown in this and other studies,[13−15] CNTs.

For these reasons, combined utilization of CNTs and DO is of great interest to many researchers and technologists. Methods for alignment of CNTs in desired networks would facilitate the assembly of highly efficient nanoscale electronic devices. Xu et al. report developments in alignment of CNTs using DNA hybridization for application in field effect transistors and other devices.[16−19] Though there have been many reports of other techniques to align CNTs, such as layer-by-layer,[20,21] Langmuir−Blodgett,[21] spin-coating,[22] and microcontact printing,[23] there has not been much experimental success in achieving alignment at the single-molecule level. To the best of our knowledge, only two approaches to the self-assembly of CNTs onto DO nanostructures have been reported. Zhao and Maune et al. separately reported on alignment of SWCNTs onto DO utilizing DNA−DNA hybridization,[13,14] and Eskelinen et al. developed a binding method using the streptavidin−biotin interaction.[15] Both of these approaches are very important because they provide highly orthogonal methods for directing CNT placement; however, multiple processing steps and specific DNA modifications are required, and only moderate yield is obtained.[13−15] In comparison to other lithographic protocols, such as dip-pen and electron beam lithography, DNA-directed molecular self-assembly may provide an efficient and cost-effective alternative. However, various problems must be addressed, including accuracy in alignment, low yield, and reproducibility.

Aqueous solubilization of CNTs is a prerequisite for the interaction of CNTs with DO templates. Chemical modification of CNTs can be used to improve CNT solubility in water and limit aggregation, but such modifications can impact the electrical and optical properties of the tubes.[24] Another method to improve the solubility is non-covalent interaction of CNTs with materials such as surfactants,[25] organic polymers,[26] and single-stranded DNA (ssDNA).[27] These modifications, in some

Received: December 13, 2012
Published: February 5, 2013

dx.doi.org/10.1021/ja312191a | J. Am. Chem. Soc. 2013, 135, 2451−2454

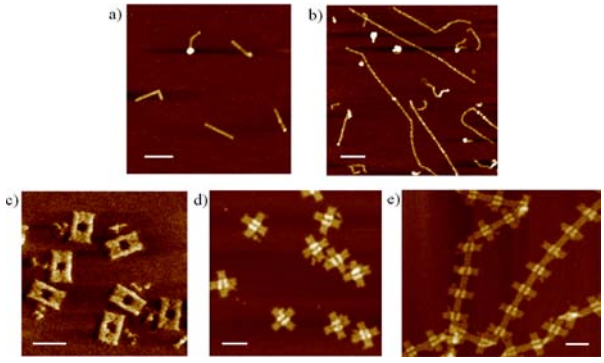

Figure 1. AFM images of (a) short SWCNTs, (b) long 6,5-SWCNTs, (c) single rectangular DO (srDO), (d) single cross DO (scDO), and (e) one-dimensional cross DO (1DcDO). Scale bar, 100 nm.

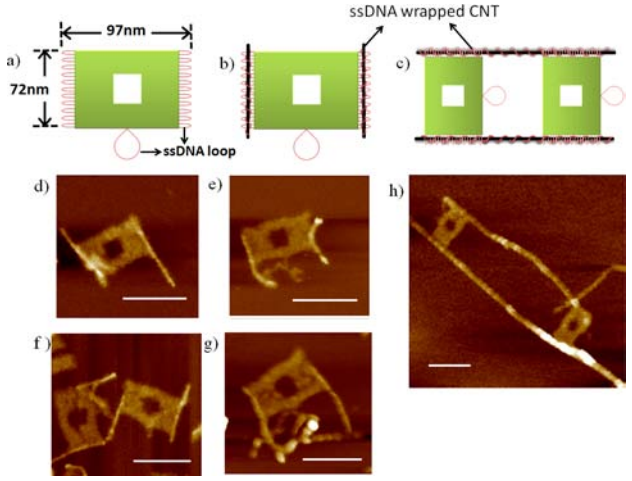

Figure 2. (Top) Schematic illustrations of (a) rectangular DO and b) and c) represent the site-specific immobilization of ssDNA-wrapped (b) short and (c) long CNTs onto srDO. (Bottom) AFM images of CNTs self-assembled onto srDO: (d–f) two CNTs aligned at the edge of srDO; (g) a third CNT immobilized onto the ssDNA loop at the bottom of the srDO; and (h) two srDOs aligning two long 6,5-SWCNTs. Scale bar, 100 nm.

cases, preserve the original properties of the CNTs without any permanent alteration. Therefore, we have adapted the ssDNA wrapping technique to disperse and separate the CNTs used in this study. The aromatic bases of ssDNA wrap around the CNT surface, which is enabled via $\pi-\pi$ bonding, and the anionic phosphate group enhances CNT solubility, leading to the formation of highly soluble DNA-coated CNTs.[27−29] Unoccupied surface regions of DNA-coated CNTs, vacated through equilibrium processes or strand displacement processes, can serve as non-covalent binding sites to allow immobilization of the CNTs onto DO platforms, presenting ssDNA-rich areas of the uncomplemented plasmid backbone.

We report here a very simple method, utilizing the mechanisms described above, to immobilize the CNTs onto DO templates. We used different shapes of DO, such as single rectangular DO (srDO), single cross DO (scDO), and one-dimensional (1D) arrays of cross DO (1DcDO) structures, for this study. Single and 1D DOs were prepared with their edges consisting of ssDNA. Two different lengths of SWCNTs (short, ~92 ± 24 nm; long, 314 ± 249 nm) were wrapped with ssDNA (GT_{20}) and T_{40} respectively, using reported protocols.[30,14] By thermal annealing, we were able to self-assemble the CNTs onto DO with a moderate yield. 1DcDO was used to align pairs of CNTs in excess of 500 nm long at fixed separation and in parallel orientation. This method does not require the DNA modification steps or gel purification necessary in the other reported protocols.

Nanotube and DNA Origami Components. Solubilization of CNTs in aqueous solution using DNA wrapping is a simple and cost-effective technique, requiring minimal instrumentation to dissolve and, more importantly, separate single CNTs from bundles. Atomic force microscopy (AFM) images of the short SWCNTs are shown in Figure 1a. Without DNA treatment, these CNTs precipitate rapidly from aqueous solutions—the ones shown here have been solubilized using $(GT)_{20}$ ssDNA. AFM image analysis indicates that the lengths range from 68 to 116 nm. The long 6,5-SWCNTs were dissolved using T_{40} ssDNA strands (Figure 1b) and display a range of lengths from 65 to 563 nm.

We used m13mp18 ssDNA plasmid (7249 bp) and short complementary DNA staple strands to program the shape of the DO as starting materials for all three DO variants. In all cases, preformed DO and prewrapped CNTs were mixed and reannealed in a thermocycler from 45 to 20 °C at the rate of 1 °C/h in order to achieve site-specific immobilization. We designed 97 nm × 72 nm srDO with a 22 nm × 26 nm landmark window in the center, as can be seen in the AFM topography image in Figure 1c. Two rectangular (97 nm × 38 nm) tiles formed from a single plasmid bind perpendicularly with each other and form scDO (Figure 1d).[31] In designing the 1DcDO (Figure 1e), we added complementary sticky-end DNA staples (sequences provided in the Supporting Information) at the ends of the arms of scDOs such that the single DO units bind each other only along one direction.

CNT Immobilization on Single Origami Constructs. The srDO constructs were prepared for CNT binding by deleting complements to short domains of the M13 plasmid at the two short edges of the structure, giving these edges ssDNA-rich areas which can immobilize and align SWCNTs at fixed distances with a parallel orientation. Figure 2a is an illustrative diagram of srDO, where green and red represent double-stranded DNA (dsDNA) and ssDNA portions of the srDO platform, respectively. The black rod with red loops represents the ssDNA-wrapped SWCNTs. Figure 2b,c illustrates binding geometries where ssDNA-wrapped short and long CNTs self-assemble with srDO. In the case of long CNTs, multiple srDOs could bind side-by-side at high packing efficiency (high binding per length of CNT available); however, this is not observed, presumably due to electrostatic repulsion between origami constructs.

AFM topography images presented in Figure 2d–f show SWCNTs successfully aligned on srDOs as designed. Although we have observed moderate yield for CNTs attached on both sides of srDO (12%, Table 1), one-side attachment (16%), misplacement, and in some cases no attachment of CNTs were also observed (Figure S1). One confounding aspect of the current origami design is that there is a long ssDNA (1480bp) loop on one of the long edges of the srDO construct, which leads in many cases to this misplacement. An example of this interference with alignment is shown in Figure 2g. Long CNTs can accommodate more than one srDO (Figure 2h), and a small number of single CNTs with a few srDO attached were also observed (Figure S2). We posit that the ssDNA-rich edges of DO provides multiple, geometrically stable binding sites which compete effectively against the single-stranded solubilization

dx.doi.org/10.1021/ja312191a | J. Am. Chem. Soc. 2013, 135, 2451−2454

Table 1. Immobilization of SWCNTs onto Origami[a]

origami	no. of binding sites	SWCNT length	no. of origami	attachment sides				
				four	three	two	one	other[b]
srDO	2	short	217	n/a	n/a	26 (12%)	34 (16%)	157 (72%)
		long	312	n/a	n/a	6 (2%)	31 (10%)	275 (88%)
scDO	4	short	168	0	3 (2%)	28 (16%)	39 (23%)	98 (58%)
		long	182	0	2 (1%)	18 (10%)	53 (29%)	109 (60%)

[a]Well-aligned CNTs on DO are counted only when attached tubes are parallel to appropriate edges of the origami construct. n/a = not applicable; experiments were not attempted or outcomes were incompatible with the design. [b]Failed products, including misalignment, misplacement, or no CNTs attached.

species for binding to CNTs via $\pi-\pi$ interaction between the bases of the ssDNA and CNTs. We have observed that binding of CNTs to origami constructs can occur at room temperature; however, thermal annealing enhances this process.

For testing CNT-DO site-specific immobilization phenomena on more than two binding sites per DO, we used the scDO platform. We prepared the scDO without staple strands complementary to the M13 plasmid at each scDO edge (Figure 3a), which provides four extended binding sites for CNTs, as illustrated in Figure 3b. As with the srDO, more than one cross origami could bind with the long 6,5-SWCNTs (Figure 3c). Figure 3d,e shows two CNTs successfully aligned on srDOs, whereas Figure 3f,g shows one CNT aligned. Even though we have observed moderate yield for CNTs attached on scDO (two CNTs, 16%; one CNT, 23%; see Table 1), misalignment in the scDO case is also driven by an unhybridized tail of excess single-stranded plasmid DNA, a 544 bp loop not used in the design (Figure 3a). The tail region causing this misalignment is often obscured (Figure S3). When scDOs were annealed with long CNTs, multiple scDOs attached to individual tubes, and in some cases these multiple scDOs led to the parallel arrangement of CNTs, as shown in Figure 3h. Multiple scDOs bound to long CNTs were often observed (Figure S4a–c). With increasing CNT concentration, the number of CNT-bound constructs increased. However, agglomeration into extended networks of cross-linked CNTs also increased, limiting the yield (Figure S4d).

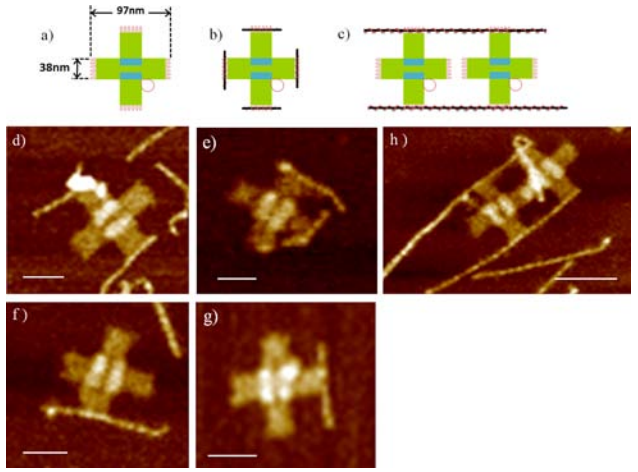

Figure 3. (Top) Schematic illustrations of (a) scDO and self-assembled scDOs with (b) short CNTs and (c) long 6,5-SWCNTs. (Bottom) AFM images of self-assembled scDOs with (d–g) short CNTs and (h) long 6,5-SWCNTs. Scale bar, 50 nm.

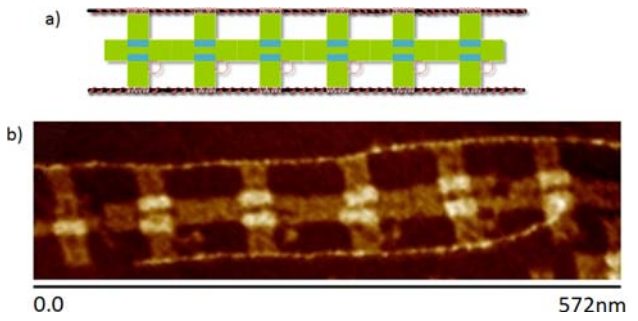

Figure 4. (a) Schematic illustration of self-assembled 1DcDO. (b) AFM image of long 6,5-SWCNTs.

CNT Immobilization on 1D Array of Origami Constructs. Though we have shown some success in aligning two long CNTs at fixed distances using either the srDO or the scDO platform, the flexibility of CNTs is so great that periodic reinforcement of their trajectory is necessary to ensure parallel arrangement over long distances. To address this problem and more accurately align the CNTs with specific distance gap, we used 1DcDO prepared without complements to short domains of the M13 plasmid at the edges of the arms of the cross not involved in polymerization. These edges have ssDNA-rich areas which can be used to bind SWCNTs at a fixed distance with parallel orientation. Arrays of these origami presenting long ssDNA-rich areas along two parallel edges enable strong attachment of long CNTs on each side of 1DcDO, as shown schematically in Figure 4a. AFM observation shows that long CNTs were successfully aligned using these 1DcDO constructs. In some cases, single CNTs bind along one edge of 1DcDO constructs as well (Figure S5).

Quantitative analysis of the alignment yield of CNTs on DO was performed, and the results are summarized in Table 1. While 12% of short srDO presents aligned CNTs bound to both srDO sides, this rate is higher for scDO (16%). In the case of 1DcDO, the yield is not readily quantified due to significant cross-linking (CNTs bridging noncontiguous origami, as discussed below). An estimate, based on limited observations, is that 2% of observed origami are bound by two CNTs in the 1DcDO case. The yield analysis presents only "simple" cases, i.e., those expected to be less susceptible to experimental artifacts, particularly sampling artifacts. Several caveats must accompany this yield listing, because the sampling is not ideal. AFM is an excellent imaging technique; however, when used in air imaging mode, AFM depends on the ability of a mica surface to capture, in a manner reflecting solution populations, objects of interest and to maintain this binding through a rather vigorous, salt-removing washing process. This constitutes an adhesion test which may bias results toward objects of lower complexity and/or higher planarity (greater surface contact). Particularly when longer

dx.doi.org/10.1021/ja312191a | J. Am. Chem. Soc. 2013, 135, 2451–2454

CNTs or longer annealing times were used, "tangles" (aggregates) were observed in this work (and reported in ref 13). These structures, which were not well imaged via AFM, are 3D random CNT networks with nodes defined by origami tiles. Yields for samples containing these highly cross-linked long nanotubes could not be reliably obtained. Such cross-linking/networking was much less prominent when short nanotubes were employed. Even in studies employing "short" nanotubes, the four-armed system (scDO) may display, for example, no full occupancy (four CNTs) instances due to (i) steric interference effects (tubes interfering with the near approach of other tubes), (ii) the attendant departure from planarity inherent in this form, which may limit adherence of the construct to the surface of the mica substrate, or (iii) kinetic effects, since only relatively short reaction times were employed. In view of these many potential artifacts, the yields in Table 1 may be lower limits, and with enhanced experimental design, higher yields, even for quite similar systems, may be anticipated.

Reported single-nanotube placement yields range from 50%[14] to 27%,[15] while yields for the placement of two tubes at two sites have been reported to range from 50%[13] to 5−6%.[14,15] It is interesting to note that, if yield is limited by kinetic factors, then future experiments using immobilized origami, which are not susceptible to aggregation, may provide a pathway to addressing the large yield deficits, which strongly impacts the technological applicability of any of these immobilization methods.

In summary, CNTs were successfully directed to self-assemble and align at the edges of origami constructs with orientation and distance of separation fixed by design. Two DO platforms with different shapes and two different sizes of CNTs were used to demonstrate this new mode of origami−CNT attachment under nonstringent conditions. In this approach, DO edges have ssDNA-rich sides which enable binding parallel to the edges via $\pi-\pi$ interactions between bases of the ssDNA and the CNTs. In addition to working as a platform to align CNTs, the DO also fixes the distance between the CNTs, as evidenced by the ability of srDO and scDO to align CNTs at spacing of ∼100 nm. With long CNTs, variable numbers of origami can be attached, at variable separations. Multiple DOs were observed on single tubes, and in some cases multiple single DO bridged two CNTs. Remarkably, using a linear array of origami constructs, an assembly consisting of two parallel CNTs was constrained to a separation of ∼100 nm over a distance of more than 500 nm. This result shows the beginnings of a future path to align semiconductor or metallic CNTs at specific separations and orientations using large DNA nanostructures, thus bridging the nanometer to micrometer size domains. Extension of this work in our laboratory is directed toward development of opto-electronic and electrochemical sensors.

■ ASSOCIATED CONTENT

Supporting Information

Experimental details and Figures S1−S7. This material is available free of charge via the Internet at http://pubs.acs.org.

■ AUTHOR INFORMATION

Corresponding Author

rahmanm@marshall.edu

Author Contributions

§A.M. and M.R. contributed equally.

Notes

The authors declare no competing financial interest.

■ ACKNOWLEDGMENTS

This work was funded by ARO awards W911NF-08-1-0109, W911NF-09-1-0218, and W911NF-11-1-0024, and NSF Cooperative Agreement EPS-1003907. The authors thank to Dr. Ming Zheng at NIST for supplying short SWCNTs, Chirag Patel, Biomedical Science, Marshall Univerity, for assistance with AFM imaging, and David Neff, Molecular and Biological Imaging Center, Marshall University, for insightful discussions.

■ REFERENCES

(1) Iijima, S. *Nature* **1991**, *354*, 56.
(2) Baughman, R. H.; Zakhidov, A. A.; de Heer, W. A. *Science* **2002**, *297*, 787.
(3) Wang, X.; Li, Q.; Xie, J.; Jin, Z.; Wang, J.; Li, Y.; Jiang, K.; Fan, S. *Nano Lett.* **2009**, *9*, 3137.
(4) Ajayan, P. M. *Chem. Rev.* **1999**, *99*, 1787.
(5) Eder, D. *Chem Rev* **2010**, *110*, 1348.
(6) Campbell, J. F.; Tessmer, I.; Thorp, H. H.; Erie, D. A. *J. Am. Chem. Soc.* **2008**, *130*, 10648.
(7) Seeman, N. C. *Nature* **2003**, *421*, 427.
(8) Rothemund, P. W. *Nature* **2006**, *440*, 297.
(9) Shen, W.; Zhong, H.; Neff, D.; Norton, M. L. *J. Am. Chem. Soc.* **2009**, *131*, 6660.
(10) Fu, J.; Liu, M.; Liu, Y.; Woodbury, N. W.; Yan, H. *J. Am. Chem. Soc.* **2012**, *134*, 5516.
(11) Kuzyk, A.; Schreiber, R.; Fan, Z.; Pardatscher, G.; Roller, E.-M.; Hogele, A.; Simmel, F. C.; Govorov, A. O.; Liedl, T. *Nature* **2012**, *483*, 311.
(12) Ko, S. H.; Gallatin, G. M.; Liddle, J. A. *Adv. Funct. Mater.* **2012**, *22*, 1015.
(13) Zhao, Z.; Liu, Y.; Yan, H. *Org. Biomol. Chem.* **2013**, *11*, 596.
(14) Maune, H. T.; Han, S. P.; Barish, R. D.; Bockrath, M.; Iii, W. A.; Rothemund, P. W.; Winfree, E. *Nat. Nanotechnol.* **2010**, *5*, 61.
(15) Eskelinen, A. P.; Kuzyk, A.; Kaltiaisenaho, T. K.; Timmermans, M. Y.; Nasibulin, A. G.; Kauppinen, E. I.; Torma, P. *Small* **2011**, *7*, 746.
(16) Xu, P. F.; Noh, H.; Lee, J. H.; Cha, J. N. *Phys. Chem. Chem. Phys.* **2011**, *13*, 10004.
(17) He, P.; Dai, L. *Chem. Commun.* **2004**, 348.
(18) McLean, R. S.; Huang, X.; Khripin, C.; Jagota, A.; Zheng, M. *Nano Lett.* **2006**, *6*, 55.
(19) Chen, Y.; Liu, H.; Ye, T.; Kim, J.; Mao, C. *J. Am. Chem. Soc.* **2007**, *129*, 8696.
(20) Mamedov, A. A.; Kotov, N. A.; Prato, M.; Guldi, D. M.; Wicksted, J. P.; Hirsch, A. *Nat. Mater.* **2002**, *1*, 190.
(21) Paloniemi, H.; Lukkarinen, M.; Aaritalo, T.; Areva, S.; Leiro, J.; Heinonen, M.; Haapakka, K.; Lukkari, J. *Langmuir* **2006**, *22*, 74.
(22) Cueto, E.; Ma, A. W. K.; Chinesta, F.; Mackley, M. R. *Int. J. Mater. Form.* **2008**, *1*, 89.
(23) Choi, S. W.; Kang, W. S.; Lee, J. H.; Najeeb, C. K.; Chun, H. S.; Kim, J. H. *Langmuir* **2010**, *26*, 15680.
(24) Banerjee, S.; Hemraj-Benny, T.; Wong, S. S. *Adv. Mater.* **2005**, *17*, 17.
(25) O'Connell, M. J.; Bachilo, S. M.; Huffman, C. B.; Moore, V. C.; Strano, M. S.; Haroz, E. H.; Rialon, K. L.; Boul, P. J.; Noon, W. H.; Kittrell, C.; Ma, J.; Hauge, R. H.; Weisman, R. B.; Smalley, R. E. *Science* **2002**, *297*, 593.
(26) Dieckmann, G. R.; Dalton, A. B.; Johnson, P. A.; Razal, J.; Chen, J.; Giordano, G. M.; Munoz, E.; Musselman, I. H.; Baughman, R. H.; Draper, R. K. *J. Am. Chem. Soc.* **2003**, *125*, 1770.
(27) Zheng, M.; Jagota, A.; Semke, E. D.; Diner, B. A.; McLean, R. S.; Lustig, S. R.; Richardson, R. E.; Tassi, N. G. *Nat. Mater.* **2003**, *2*, 338.
(28) Tu, X.; Manohar, S.; Jagota, A.; Zheng, M. *Nature* **2009**, *460*, 250.
(29) Khripin, C. Y.; Arnold-Medabalimi, N.; Zheng, M. *ACS Nano* **2011**, *5*, 8258.
(30) Huang, X.; McLean, R. S.; Zheng, M. *Anal. Chem.* **2005**, *77*, 6225.
(31) Liu, W.; Zhong, H.; Wang, R.; Seeman, N. C. *Angew. Chem., Int. Ed.* **2011**, *50*, 264.